Proceedings of IMECE2007
2007 ASME International Mechanical Engineering Congress and Exposition
November 11–15, 2007, Seattle, Washington, USA

IMECE2007-41988

CONDITION MONITORING OF OPERATING SPINDLE BASED ON STOCHASTIC SUBSPACE IDENTIFICATION

Robert X. Gao
Dept. of Mechanical and Industrial Engineering
University of Massachusetts
Amherst, MA 01003
Email: gao@ecs.umass.edu

Ruqiang Yan
Dept. of Mechanical and Industrial Engineering
University of Massachusetts
Amherst, MA 01003
Email: ryan@ecs.umass.edu

Li Zhang
Global Research Center
General Electric Corporation
Niskayuna, NY 12309
Email: li.zhang@research.ge.com

Kang B. Lee
Manufacturing Metrology Division
National Institute of Standards and Technology
Gaithersburg, MD 20899
Email: kang.lee@nist.gov

ABSTRACT

Accurate identification of spindle modal parameters is critical to realizing a new generation of "smart" machine tools with built-in self-diagnosis capability. This paper describes a new approach to extracting spindle modal parameters from the output measured during operation, based upon stochastic subspace identification. The technique accounts for structural dynamic behavior, associated with the spindle rotation, that is not present when the spindle remains stationary. Experimental results conducted on a customized spindle test bed under different speed-load combinations confirm the effectiveness of the new technique for on-line spindle condition monitoring.

KEYWORDS: condition monitoring, non-intrusive testing, spindle, structural dynamics, subspace identification

1. INTRODUCTION

Spindles are essential elements in virtually all machine tools and their structural dynamic behavior directly affects the performance of machine tools. Identification of spindle modal parameters has been extensively investigated, and various analytical and experimental methods have been explored. For example, lumped mathematical models were applied to derive guidelines for improving the dynamics of machine tools [1]. Receptance coupling substructure analysis was used to predict the structural response of a spindle-holder assembly [2]. By combining receptance coupling analysis with beam theory [3], a spindle-holder assembly was modeled to predict chatter stability, based on the machine tool's Frequency Response Function (FRF). The FRF-based method was also developed to determine boundary conditions for stable metal removal rates in milling operation. In another study [5], the impulse responses to hammer strikes on stationary spindles were analyzed to extract various parameters such as structural stiffness, damping, and dominant mode shapes. However, dynamics captured on a stationary spindle may not adequately represent the rotating nature of the spindle, since its modal parameters (e.g., number of vibration modes and modal amplitude) may be affected by the actual operating conditions. For example, the natural frequency of a spindle was found to fluctuate with shaft speed and bearing preload [6]. Also, stiffer spring characteristics due to a higher axial bearing preload have been found to result in higher natural frequencies [7]. Although hammer-strike techniques are viable for identifying dynamic changes of a rotating spindle tool-tip for improved chatter stability predictions [8], such "intrusive" methods conflict with the normal mode of operations in industry.

This paper introduces a new non-intrusive measurement technique to enable in-process modal parameter identification on rotating spindles under varying operation conditions. Instead of fitting an empirical model to the FRF from artificial excitations (e.g., hammer strikes), the Stochastic Subspace Identification (SSI) approach [9, 10] was taken to extract modal parameters from the spindle's measured output. This technique accounts for dynamic changes caused by the rotations of the spindle without the need for artificial excitations [11], and thus does not suffer from the inherently low signal-to-noise ratio typically associated with hammer-striking a rotating spindle.

The structure of this paper is organized as follows. To illustrate the difference between modal analyses for stationary and rotational conditions, Section 2 presents the results of spindle mode identification based on hammer-strike tests on a spindle test bed. The theory related to the SSI-based technique is introduced in Section 3. This technique utilizes the measured spindle vibration outputs to identify mode parameters which have shown to be comparable to those obtained using traditional methods. The application of the new technique for monitoring an operating spindle is experimentally verified in section 4. Finally, conclusions are drawn in section 5.

2. SPINDLE MODE IDENTIFICATION

A series of modal analysis experiments was performed on a customized spindle test bed to establish an experimental basis for extracting the spindle modal parameters. As shown in Figure 1, an air cylinder applies a constant force to the spindle as the static preload. A dynamic load cylinder applies impulsive forces to the spindle shaft, as a means to accelerate the structural deterioration process of the spindle and establish a spindle service life history. The test bed was supported by four 42 mm-angular contact ball bearings mounted as duplex pairs on each end of the spindle shaft. The sampling frequency of the data acquisition board was set at 20 kHz, with the cut-off frequency of the anti-aliasing filter being 10 kHz.

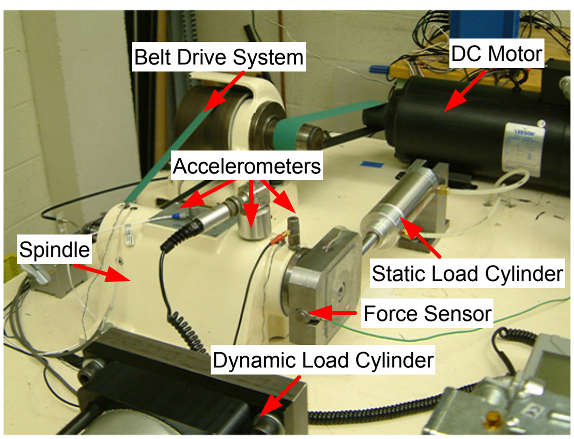

Figure 1. Spindle test bed setup

Using an instrumented hammer, strike-based tests to excite spindle resonance modes were first performed with the spindle stationary. The same tests were then repeated with the spindle rotating at 126 rad/s (1,200 rpm). Four accelerometers were placed on the spindle to measure the vibrations. To estimate the spindle's FRF, coherence functions were calculated to relate the known input forces from hammer strikes to the output measurements. The coherence function provides a measure of the degree of correlation between each frequency component of the input and the output signals, thereby establishing the statistical validity of the spindle FRF. The closer the coherence value is to 1, the more accurate the estimated FRF will be.

While the coherence function for the stationary spindle indicates a strong correlation between the input and output signals across the entire spectrum, as shown in Figure 2a, it fluctuates significantly for the rotating spindle (Figure 2b). In addition, the average coherence value across the frequency range for the rotating spindle is less than 0.5, indicating a weak correlation between the input and output signals. This is due to contaminations from the spindle's structure-borne vibrations. Consequently, the measured data could not be used to derive a valid FRF. To improve the signal-to-noise ratio (SNR), the dynamic load cylinder was utilized to provide stronger impulsive force inputs to the spindle than the hammer strikes. The coherence function shown in Figure 2d indicates significantly improved correlation between the input force and output measurement as compared to that in Figure 2b, with the average coherence value approaching 1. As a result, air cylinder strikes were used to estimate the FRF of spindle in both the stationary and rotating conditions.

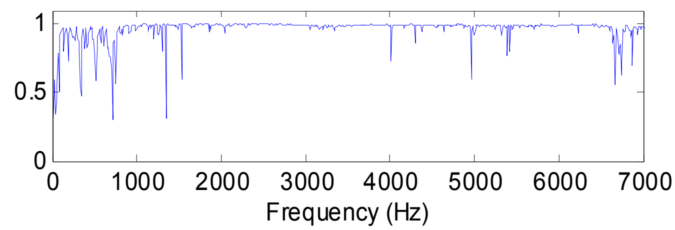

(a) Hammer strike on stationary spindle

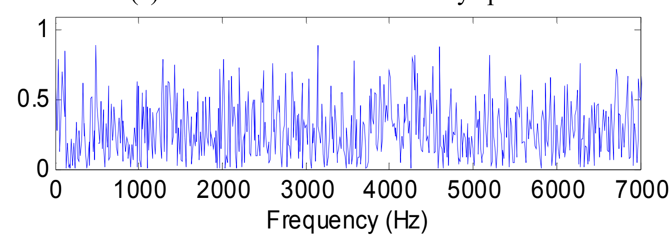

(b) Hammer strike on rotating spindle

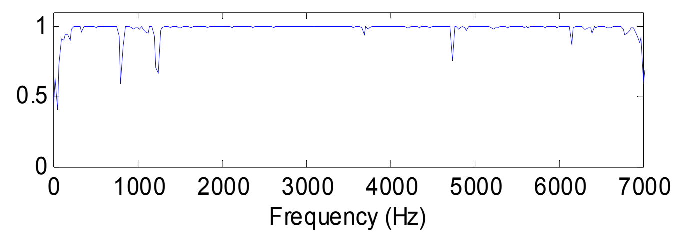

(c) Cylinder strike on stationary spindle

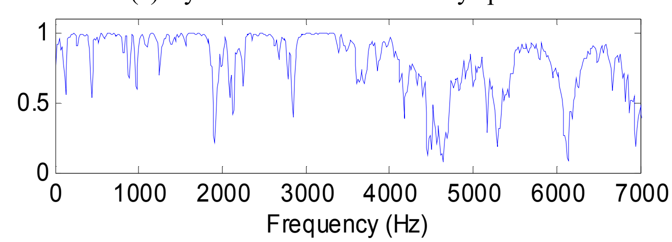

(d) Cylinder strike on rotating spindle

Figure 2. Coherence functions obtained from the modal analysis of four experimental conditions

The results of the FRF, which is estimated using the Rational Fraction Polynomials (RFP) method [12], are shown in Figure 3. Three major structural modes (denoted as ❶, ❷ and ❹) are identified for the stationery spindle in the frequency range from 2,000 Hz to 7,000 Hz. In comparison, the spectrum for the rotating spindle revealed an additional mode at approximately 5,200 Hz, denoted as ❸ in Figure 3b. This indicates the drawback of traditional modal analysis techniques in possibly missing certain dynamic characteristics of a rotating spindle, and illustrates the need for spindle dynamics identification under actual operating conditions.

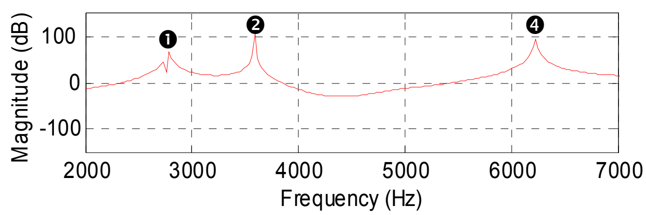

(a) Cylinder strike on stationary spindle

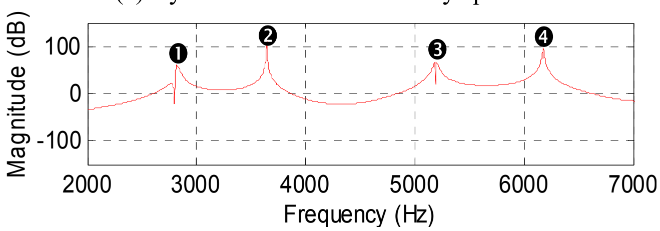

(b) Cylinder strike on rotating spindle

Figure 3. Frequency response functions using both input and output measurements

3. STOCHASTIC SUBSPACE IDENTIFICATION

Striking a rotating spindle is invasive and generally not acceptable in production due to interference and potential damage to the machine tool. This motivated the development of a new non-invasive technique for spindle modal analysis. Such a technique can be based on the Stochastic Subspace Identification (SSI) method, which extracts spindle modal parameters from its measured vibrations. The technique is described below.

Assuming that the vibrational behavior of a continual mechanical system (such as a spindle) can be analytically approximated by that of an equivalent, multiple degree-of-freedom (MDOF) system (e.g., a series of mass-spring-dampers), and that the structural response is linear and time-invariant, the discrete state-space model of the spindle can then be expressed as:

$$x_{k+1} = Ax_k + Bu_k + w_k \tag{1}$$

$$y_k = Cx_k + Du_k + v_k \tag{2}$$

where $x_k = x(k\Delta t)$ is the discrete-time state vector, u_k is the structural input displacement vector resulting from a known excitation force, y_k is the system response vector, A is the state matrix, B is the input matrix, C is the output matrix, and D is the direct transmission matrix. The two components, w_k and v_k, represent the disturbance noise to the spindle and measurement noise due to sensor inaccuracy, respectively, and are stochastic in nature. The state space dimension n is determined by the number of independent variables needed to describe the physical system, i.e., the number of mass-spring-dampers as the constituent elements for spindle modeling. If no excitation force is applied to the spindle, the term u_k vanishes, and the system can then be represented by the stochastic state-space model as [10, 11]:

$$x_{k+1} = Ax_k + w_k \tag{3}$$

$$y_k = Cx_k + v_k \tag{4}$$

Equation (3) indicates that the new state of the spindle physical system, x_{k+1}, can be obtained by the sum of the state matrix A ($n\times n$) multiplied by the old state vector x_k ($n\times 1$) and the disturbance noise vector w_k ($n\times 1$). As a result, the dynamics of the spindle is completely characterized by the state matrix A, and the modal parameters can then be extracted from its eigenvalues. As shown in Eq. (4), the measured system response vector y_k ($m\times 1$) contains the observable part of the state vector Cx_k ($m\times 1$) and the measurement noise vector v_k ($m\times 1$), with m being the number of sensors used for the measurements. In order to identify the state matrix A from the measured system response (vibrations of the spindle), an optimal estimate of the state-space model must be obtained based on the measured system response. In the stochastic framework, the measured system response must be a Gaussian stochastic process with zero mean ($E[y_k]=0$) and characterized by the output covariance matrix $E[y_{k+i} \quad y_k^T] = \Lambda_i$ This implies that the input noise processes w_k and v_k are also zero-mean Gaussian ($E[w_k]=0$ and $E[v_k]=0$) with covariance matrices defined as:

$$E\left[\begin{pmatrix} w_p \\ v_p \end{pmatrix}\begin{pmatrix} w_q^T & v_q^T \end{pmatrix}\right] = \begin{pmatrix} Q & S \\ S^T & R \end{pmatrix}\delta_{pq} \tag{5}$$

where δ_{pq} is the Kronecker delta function, and Q, S, and R are the noise covariance matrices. Similarly, the state vector x_k is also zero-mean ($E[x_k]=0$) with the state covariance matrices and the updated state-output matrices defined using the noise covariance matrices as:

$$E[x_k x_k^T] = \Sigma = A\Sigma A^T + Q \tag{6}$$

$$E[x_{k+1} \quad y_k^T] = G = A\Sigma A^T + S \tag{7}$$

Based on the covariance matrices defined in Eqs. (5) - (7), the output covariance matrices can be rewritten as:

$$E[y_{k+i} \quad y_k^T] = \begin{cases} \Lambda_0 = C\Sigma C^T + R & i = 0 \\ \Lambda_i = CA^{i-1}G & i \neq 0 \end{cases} \tag{8}$$

These covariance matrices describe the stochastic properties of the state-space systems, and can be used to estimate the state-space model, and subsequently, to identify the state matrix A.

Another system matrix needed for the estimation is the extended observability matrix, which is defined as:

$$O_i \equiv \begin{pmatrix} C \\ CA \\ CA^2 \\ \cdots \\ CA^{i-1} \end{pmatrix} \quad (9)$$

Two approaches can be employed for state-space model estimation: data-driven and covariance-driven algorithms [10]. For this study, a reference-based data-driven algorithm was investigated. Kalman filtering was employed for the optimal prediction of the state vector x_{k+1} by making use of the chosen reference sensor measurements denoted as $\hat{x}_{k+1}$. A Kalman filter state sequence can be formed by the various Kalman filter state estimates as:

$$\hat{X}_i \equiv (\hat{x}_i \; \hat{x}_{i+1} \cdots \hat{x}_{i+j-1}) \quad (10)$$

Once the Kalman filter state estimates are obtained, numerical techniques can be applied to estimate the state-space model, e.g., by using the QR-factorization technique [10], which essentially projects the row space of the future outputs into the row space of the past outputs. The projection can be factorized as the product of the observability matrix and the Kalman filter state sequences:

$$P_i = O_i \hat{X}_i \quad (11)$$

Thus, the Kalman filter state sequence is expressed as:

$$\begin{cases} \hat{X}_i = O_i^{-1} P_i \\ \hat{X}_{i+1} = O_{i+1}^{-1} P_{i+1} \end{cases} \quad (12)$$

By applying Eq. (12) and extending Eqs. (3) and (4), the state-space spindle model is then obtained in the form of a set of linear equations:

$$\begin{pmatrix} \hat{X}_{i+1} \\ Y_{i|i} \end{pmatrix} = \begin{pmatrix} A \\ C \end{pmatrix} \hat{X}_i + \begin{pmatrix} \rho_w \\ \rho_v \end{pmatrix} \quad (13)$$

where $Y_{i|i}$ is the measured system responses written in the form of a block Hankel matrix, and $(\rho_w, \rho_v)^T$ are the residuals. Since the residuals are uncorrelated with $\hat{X}_i$, the system matrices A and C can be solved using Eq. (13) as:

$$\begin{pmatrix} A \\ C \end{pmatrix} = \begin{pmatrix} \hat{X}_{i+1} \\ Y_{i|i} \end{pmatrix} \hat{X}_i^{-1} \quad (14)$$

Since the dynamic behavior of the spindle is represented by the state matrix A, the eigen-frequencies and modal damping ratios can be obtained from the eigenvalues of state matrix A, using known decomposition techniques.

In essence, the SSI algorithm assumes that the input noise drives a virtual loading system to generate force input to the structure of interest, e.g., the spindle, as illustrated in Figure 4.

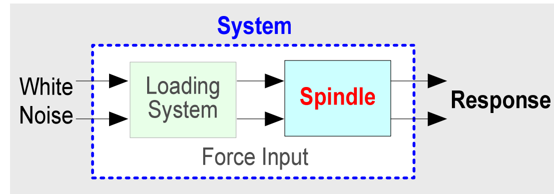

Figure 4. Illustration of output-only identification system

With this representation, the identification process includes not only the vibration modes associated with the structure itself, but also the modes that belong to the virtual loading system. To ensure correct and accurate modal identification, effective separation of the structural modes from the virtually excited modes is needed. Using such an algorithm, the structural dynamics of the rotating spindle is shown in Figure 5, based on the normal operating input from the spindle itself.

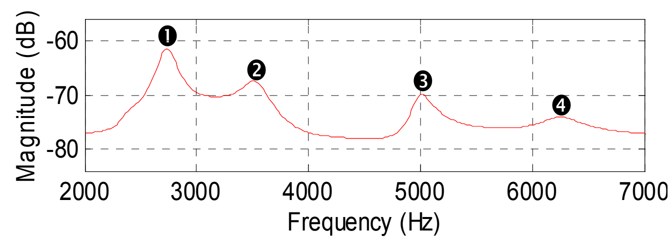

Figure 5. Frequency response function using output-only measurement

The spindle modes in Figure 5 closely match those identified using cylinder strikes on the spindle (Figure 3b). Thus the applicability of the output-only modal identification technique is confirmed. Since the developed algorithm is performed while the spindle is rotating, it allows for on-line spindle condition monitoring. Correlation with the progression of the spindle modes through its service life can provide important feedback to spindle designers, and a basis for spindle condition monitoring.

4. MONITORING OPERATING SPINDLE

A series of experiments was conducted on the test bed to evaluate the applicability of the new SSI technique for spindle condition monitoring. To accelerate degradation of the spindle structure, dynamic impacts with amplitude of 13,300 N were applied to the spindle shaft rotating at 377 rad/s (3,600 rpm). The time interval for the two successive impacts was set to 1 second. While for Stochastic Subspace Identification the input noise terms are usually assumed to be white, it was observed in preliminary experiments that the spindle dynamics also contains certain dominant frequency components, such as its rotational frequency and bearing characteristic frequencies. These frequency components cannot be separated from the eigen-frequencies of the system, and thus appear as poles of the state matrix A. Since the highest dominant frequency of the spindle (i.e., the ball passing frequency on the inner raceway, or BPFI) and its harmonics were found to be all below 2,000 Hz for the highest spindle rotational speed investigated (837 rad/s or 8,400 rpm), they were removed from the data set through high-pass filtering so that only signals within the 2,000 Hz to 10,000 Hz (Nyquist) range were analyzed.

Spindle modal parameter identification was subsequently performed using the SSI algorithm described before. Since the true model order, i.e., the exact state space dimensions of the system, is unknown, a range of candidate state space models was used. To ensure accuracy, the number of dimensions was over-specified (i.e., 80) initially, and the appropriate dimension was iteratively determined to extract the modal parameters. The estimated models were plotted in the stabilization diagram. An example of such a diagram for the measured data under 126 rad/s (1,200 rpm) speed, no static load, and with accumulated 700 dynamic impacts is given in Figure 6, where the estimated eigen-frequencies for each state space dimension are shown in red. It should be noted that noise (computational) modes are also estimated in addition to the structural modes. These noise modes are the results of the non-fulfilled assumptions made by the algorithm itself. Generally, noise modes are spread out randomly and can be eliminated by setting a threshold for the damping ratio, typically 5 %. This is because the structural modes are usually lightly damped (e.g., spindle damping ratio found to be less than 4 %) whereas the noise modes are more heavily damped. Furthermore, the structural modes would appear "stable" across the various state space dimensions with the estimated modal parameters. As shown in Figure 6, there are six stable modes presented in the diagram, between 2,000 Hz and 10,000 Hz. The modal parameters can then be obtained by finding one state space dimension where all modes are stable.

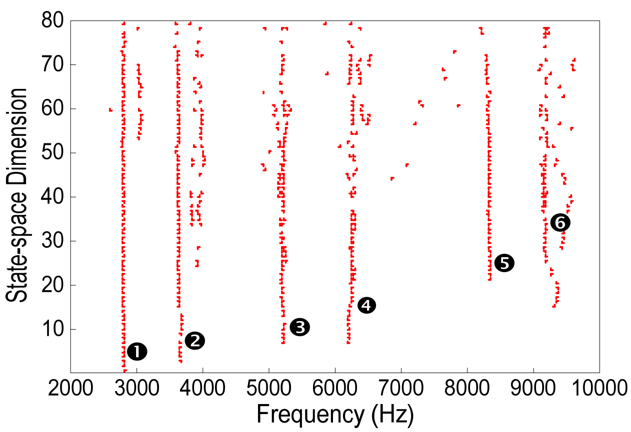

Figure 6. Stabilization diagram for the data set of 126 rad/s (1200 rpm) speed and no static load

Using the SSI method, the natural frequencies and FRFs of the spindle were estimated for data sets collected under various operating conditions. Figure 7 shows a comparison of the estimated FRFs (red-colored solid lines) with the measured FRFs (blue, dotted lines) for the data sets where the speed was 126 rad/s (1,200 rpm) and no static load was applied. Clearly the dynamic behavior of the spindle has changed as a result of the accumulated impacts. Before the impact application when the spindle was "healthy", four structural modes (denoted ❶❷❸❹) were identified, as shown in Figure 6a. As the number of impacts increased, two additional modes (denoted ❺❻) appeared in the frequency range of 8,000 Hz to 10,000 Hz. As seen in Figure 8, the magnitude of the modes increased with the number of the impacts. In particular, mode ❹ appears to have increased by about 15 dB after 1,100 impacts, as listed in Table 1. Such an increase was also confirmed when the spindle output is analyzed by an alternative technique based on the wavelet envelope spectrum [13]. It can be seen in Figure 9 that vibration frequencies are concentrated at around 6,000 Hz in the wavelet domain, corresponding to mode ❹ of the spindle. Furthermore, several frequencies associated with spindle unbalance (100 Hz and 200 Hz), bearing inner raceway defects (664 Hz), and the combined effect of spindle unbalance and inner raceway defects (764 Hz, etc.) were successfully detected, indicating the effects of the accumulated impacts.

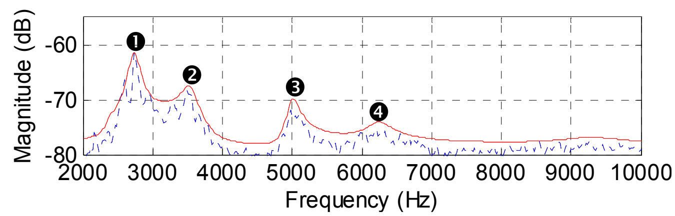

(a) Before impact test

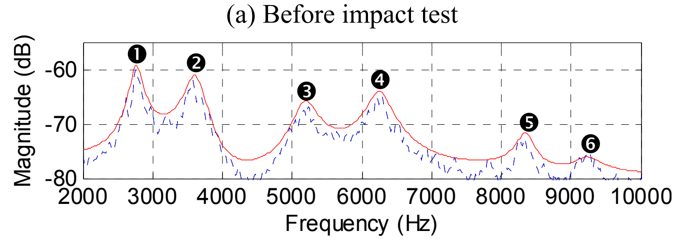

(b) After 400 impacts

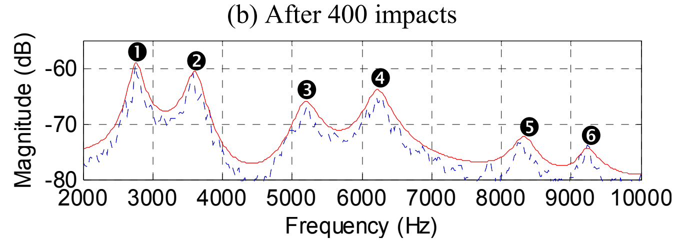

(c) After 700 impacts

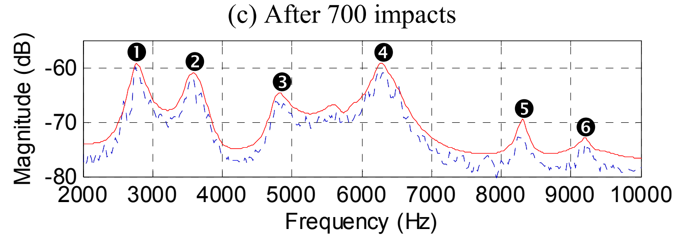

(d) After 1100 impacts

Figure 7: Comparison of estimated and measured FRFs.

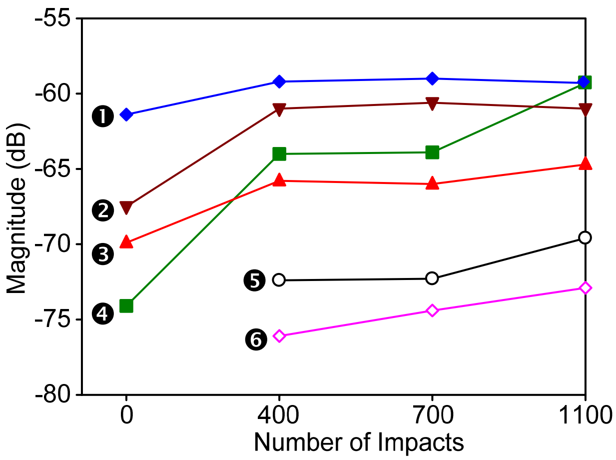

Figure 8. Magnitudes of identified modes

Table 1. Magnitude change of the identified mode❹

Mode ❹	Number of Impacts			
	0	400	700	1,100
Magnitude (dB)	-74.1	-64.0	-63.9	-59.3
Increase (dB)	-	10.1	10.2	14.8

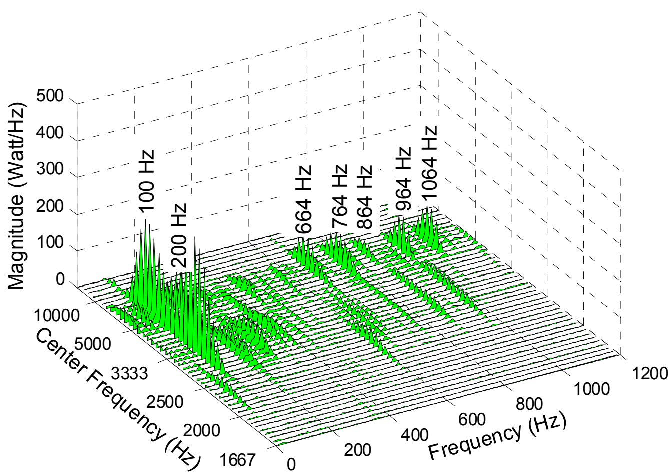

Figure 9. Wavelet envelope spectrum of the vibration signal measured after 1,100 impacts.

To specify the effect of static loading on the spindle dynamics, the natural frequencies for four loading conditions were extracted under 126 rad/s (1,200 rpm) speed. The data sets were collected after 700 impacts. It was found that for all six modes identified in Figure 7, the natural frequencies increase as the static load increases. Several examples are given in Table 2, illustrating changes of the natural frequencies for modes ❶ and ❺. Also, similar trends have been identified for other structural modes, suggesting that increased static load has led to increased stiffness of the spindle structure, as reflected in increased natural frequencies. This finding is in agreement with the investigations reported in [8] and [14].

Table 2. Effect of static load on spindle natural frequencies

Mode	Static Load (N)			
	0	420	840	1,260
❶	2,756	2,770	2,775	2,790
❺	8,289	8,300	8,320	8,390

The effect of rotational speeds on spindle natural frequencies has also been investigated. Table 3 lists the changes of the natural frequencies for mode ❶ and ❺ under four different speeds. No static load was applied to the spindle. It was noted that the natural frequencies decrease with the spindle speed. This phenomenon can be attributed to decreasing stiffness caused by centrifugal forces of the rotating spindle. This is due to the fact that, for a bearing with a fixed outer raceway, centrifugal forces would decrease the contact angle at the outer raceway of the bearing while increasing the contact angle at the inner raceway of the bearing [15]. The changed contact angle difference between outer and inner raceway reduces the stiffness of the bearing. As a result, the natural frequencies will decrease.

Table 3. Effect of speed on spindle natural frequencies

Mode	Speed: rad/s (rpm)			
	126 (1,200)	377 (3,600)	630 (6,000)	879 (8,400)
❶	2,756	2,755	2,730	2,725
❺	8,289	8,285	8,275	8,240

5. CONCLUSIONS

An SSI-based output-only modal identification technique has been developed for on-line spindle condition monitoring. This technique allows the extraction of spindle modal parameters under actual operating conditions, and does not require any hammer strikes to be applied to the spindle. From experiments conducted on a customized spindle test bed, it was found that the SSI algorithm has returned similar modal identification results to those obtained using the traditional hammer strike method. The on-line applicability of the SSI algorithm allowed identification of changing modal parameters as a result of the accumulated impacts to the spindle. The results not only provide insight into the present condition of a working spindle, but can also be used to predict its future performance, thus serving as a tool for prognosis of machine remaining service life.

ACKNOWLEDGEMENT

This work was supported by the Smart Machining Systems Program at the National Institute of Standards and Technology (NIST). Collaboration from Steven Fick of the

Manufacturing Metrology Division during the experimental study is sincerely appreciated.

REFERENCES

[1] Okubo, N. and Yoshida, Y., 1982, "Application of modal analysis to machine tool structures," *Annals of the CIRP*, Vol. 31, No. 1, pp. 243-246.

[2] Schmitz, T. L., 2000, "Predicting high-speed machining dynamics by substructure analysis," *Annals of the CIRP*, Vol. 49, No. 1, pp. 303-308.

[3] Budak, E., Ertürk, A., and Özgüven, H.N., 2006, "A modeling approach for analysis and improvement of spindle-holder-tool assembly dynamics," *Annals of the CIRP*, Vol. 55, No. 1, pp. 369-372.

[4] Smith, S. and Snyder, J., 2001, "A cutting performance based template for spindle dynamics," *Annals of the CIRP*, Vol. 50, No. 1, pp. 259-262.

[5] Altintas, Y. and Park, S. S., 2004, "Dynamic compensation of spindle integrated force sensors," *Annals of the CIRP*, Vol. 53, No. 1, pp. 305-308.

[6] Akturk, N., 2003, "Some characteristic parameters affecting the natural frequency of a rotating shaft supported by defect-free ball bearings," *Proceedings of the Institute of Mechanical Engineers, Part K: Journal of Multi-body Dynamics*, Vol. 217, No. 2, pp. 145-151.

[7] Alfares, M.A. and Elsharkawy, A.A., 2003, "Effects of axial preloading of angular contact ball bearings on the dynamics of a grinding machine spindle system," *Journal of Materials Processing Technology*, Vol. 136, pp. 48-59.

[8] Schmitz, T. L., Ziegert, J., and Stanislaus, C., 2004, "A method for predicting chatter stability for systems with speed-dependent spindle dynamics," *Transactions of NAMRI/SME*, Vol. 32, pp.17-24.

[9] Kushnir, E., 2004, "Application of operational modal analysis to a machine tool testing," *Proceedings of IMECE04*, pp. 57-62.

[10] Peeters, B. and De Roeck, G., 1999, "Reference-based stochastic subspace identification for output-only modal analysis," *Mechanical Systems and Signal Processing*, Vol. 13, No. 6, pp. 855-878.

[11] Tasker, F., Bosse, A., and Fisher, S., 1998, "Real-time modal parameter estimation using subspace methods: theory," *Mechanical Systems and Signal Processing*, Vol. 12, pp. 795-806.

[12] Richardson, M.H. and Formenti, D.L., 1982, "Parameter estimation from frequency response measurements using rational fraction polynomials," *Proceedings of the First International Modal Analysis Conference*, Orlando, FL. November 8-10, pp. 167-181.

[13] Zhang, L., Gao, R., and Lee, K., 2006, "Spindle health diagnosis based on analytic wavelet enveloping," *IEEE Transactions on Instrumentation and Measurement*, Vol. 55, No. 5, pp. 1850-1858.

[14] Altintas, Y. and Cao, Y., 2005, "Virtual design and optimization of machine tool spindles," *Annals of the CIRP*, Vol. 54, No. 1, pp. 379-382.

[15] Abele, E. and Fiedler U., 2004, "Creating stability lobe diagrams during milling," *Annals of the CIRP*, Vol. 53, No. 1, pp. 309-313.